J Syst Sci Complex (2010) 23: 379–389

A NEW SIMPLE 2-D PIECEWISE LINEAR MAP

Zeraoulia ELHADJ · Julien Clinton SPROTT

DOI: 10.1007/s11424-010-7184-z
Received: 10 September 2007 / Revised: 5 September 2009

Abstract A new simple piecewise linear map of the plane is presented and analyzed, then a detailed study of its dynamical behaviour is described, along with some other dynamical phenomena, especially fixed points and their stability, observation of a new chaotic attractors obtained via border collision bifurcation. An important result about coexisting chaotic attractors is also numerically studied and discussed.

Key words Border collision bifurcation, new chaotic attractor, piecewise linear map.

1 Introduction

The study of discrete mappings such as piecewise linear maps[1−5] is an interesting contribution to the development of the theory of dynamical systems, with many possible applications in science and engineering[6−7]. A large number of physical and engineering systems have been found that are best represented by piecewise maps[8−11] where the discrete-time state space is divided into two or more compartments with different functional forms separated by borderlines. Finding chaotic regions in discrete mappings is a very interesting field in dynamical systems theory[12−14].

The Lozi map[2] given by

$$L(x,y)=\begin{pmatrix} 1-a\,|x|+by \\ x \end{pmatrix} \tag{1}$$

has been widely studied because it is the simplest example of a dissipative piecewise linear map with chaotic solutions[2−3]. It has an area contraction that depends only on b and is thus constant over the orbit in the xy-plane. It can also be written as a time-delayed map:

$$x_{n+1}=1-a\,|x_n|+bx_{n-1}. \tag{2}$$

Here we propose and analyze an equally simple two-dimensional piecewise linear map given by

$$f(x,y)=\begin{pmatrix} 1-a\,|y|+bx \\ x \end{pmatrix}, \tag{3}$$

Zeraoulia ELHADJ
Department of Mathematics, University of Tébessa, 12002, *Algeria.*
Email: zeraoulia@mail.univ-tebessa.dz; zelhadj12@yahoo.fr.
Julien Clinton SPROTT
Department of Physics, University of Wisconsin, Madison, WI 53706, *USA.* Email: sprott@physics.wisc.edu.

where a and b are bifurcation parameters. Equation (3) is an interesting system having simple form, similar to the Lozi map[2], but with the time delay in the piecewise linear rather than in the linear term as evidenced by writing it in the time-delayed form:

$$x_{n+1} = 1 - a\,|x_{n-1}| + bx_n\ . \tag{4}$$

Despite its apparent similarity and simplicity, it differs from the Lozi map in that it has a much wider variety of attractors. Whereas the attractors for the Lozi map are qualitatively similar, all the attractors for the system (3) with regular basins of attraction, have either dimension 2 (if chaotic) or 0 (if not) for both the Kaplan-Yorke dimension and the correlation dimension except perhaps for a set of measure zero in the parameter space at the bifurcation boundaries.

The associated function $f(x, y)$ of map (3) is continuous on $\mathbb{R}^2$, but it is not differentiable at the point $(x, y = 0)$, for all $x \in \mathbb{R}$, and it is a diffeomorphism when $a \neq 0$, since the determinant of its Jacobian matrix is nonzero if and only if $a \neq 0$. Due to the shape of the vector field f of map (3) the plane can be divided into two linear regions denoted by:

$$R_1 = \left\{(x, y) \in \mathbb{R}^2 /\ y < 0\right\}, \tag{5}$$

$$R_2 = \left\{(x, y) \in \mathbb{R}^2 /\ y \geq 0\right\}, \tag{6}$$

where in each of these regions the map (3) is linear.

As with the Lozi map (1), systems such as the one in Equation (3) typically have no direct application to particular physical systems, but they serve to exemplify the kinds of dynamical behavior, such as routes to chaos, which are common in physical chaotic systems. Thus, an analytical and numerical study is warranted.

2 Fixed Points and Their Stability

In this section, we begin by studying the existence of fixed points of the f mapping and determine their stability type. It is easy to see that there exists $P_1 = \left(\frac{-1}{a+b-1}, \frac{-1}{a+b-1}\right) \in R_1$ when $b > -a + 1$, and $P_2 = \left(\frac{-1}{-a+b-1}, \frac{-1}{-a+b-1}\right) \in R_2$ when $b < a + 1$. We remark that the map (3) has the same fixed points as the Lozi map (1), but with different stability types, due to differences in their Jacobian matrices. However, maps (1) and (3) are not topologically conjugate. If $b \leq -a + 1$, or $b \geq a + 1$, then P_1 or P_2 does not exist. Also, we remark that the path of the fixed points does not depend continuously on parameters a, b, and the fixed points do not touch the border $y = 0$ for all the values of a, b. Since the nature of the border collision bifurcations depends on the local character of the map in the neighborhood of the fixed point, it suffices to look at the piecewise linear approximation at the two sides of the border. It has been shown that a normal form for the piecewise system in the neighborhood of a fixed point on the border can be expressed as[14].:

$$N(x, y) = \begin{cases} \begin{pmatrix} \tau_1 & 1 \\ -\delta_1 & 0 \end{pmatrix} \begin{pmatrix} x \\ y \end{pmatrix} + \begin{pmatrix} 0 \\ 1 \end{pmatrix} \mu, \text{ if } x < 0, \\ \\ \begin{pmatrix} \tau_2 & 1 \\ -\delta_2 & 0 \end{pmatrix} \begin{pmatrix} x \\ y \end{pmatrix} + \begin{pmatrix} 0 \\ 1 \end{pmatrix} \mu, \text{ if } x > 0, \end{cases} \tag{7}$$

where μ is a bifurcation parameter, and $\tau_i, \delta_i, i = 1, 2$, are the traces and determinants of the corresponding matrices of the linearized map in the two subregions R_1 and R_2 evaluated at P_1 and P_2, respectively. For the map (3) one has:

$$\tau_1 = \tau_2 = b, \quad \delta_1 = -a, \quad \delta_2 = a, \tag{8}$$

The normal form $N(x, y)$ can be used to study local bifurcations of the original piecewise map when a fixed point collides with the border[14], but this is not the case for the map (3). In addition, the results on border collision bifurcations in two-dimensional systems available in [12–15] require that $|\delta_1| < 1$ and $|\delta_2| < 1$, which gives the condition $|a| < 1$. Finally, we cannot use the normal form theory for 2-dimensional piecewise maps to study the map (3). On the other hand, the Jacobian matrix of the map (3) evaluated at the fixed point P_1 is given by $J_1 = \begin{pmatrix} b & a \\ 1 & 0 \end{pmatrix}$, and its characteristic polynomial is given by $\lambda^2 - b\lambda - a = 0$. The Jacobian matrix of map (3) evaluated at the fixed point P_2 is given by $J_2 = \begin{pmatrix} b & -a \\ 1 & 0 \end{pmatrix}$, and its characteristic polynomial is given by $\lambda^2 - b\lambda + a = 0$. Hence, one has the following results:

The fixed point P_1 is:

i) A repeller if $a > 1, 0 < b < a - 1$;

ii) A regular saddle, if $-1 < a < 0, b > 1 - a$;

iii) A flip saddle if $0 < a < 1, b > 1 - a$.

While the fixed point P_2 is:

i) A regular attractor, if $0 < a < 1, 2\sqrt{a} < b < 1 + a$;

ii) A flip attractor if $-1 < a < 0, -1 - a < b < 1 + a$, or $0 < a < 1, -1 - a < b < -2\sqrt{a}$;

iii) A flip saddle if $-1 < a < 0,\ b < -1 - a, b < a + 1$, or $0 < a < 1,\ b < -1 - a$;

iv) A clockwise spiral attractor if $0 < a < 1,\ 0 < b < 2\sqrt{a}$;

v) A counter-clockwise spiral attractor if $0 < a < 1,\ -2\sqrt{a} < b < 0$;

vi) A repeller if $a > 1$, $b < 1 - a$.

A schematic representation of these results is given in Figure 1, where the regions $(B_i)_{0 \le i \le 7}$ have respectively the following boundaries: $b_0 = -a - 1, b_1 = a + 1, b_2 = 1 - a, b_3 = a - 1, b_4 = -2\sqrt{-a}, b_5 = 2\sqrt{-a}$, $b_6 = -2\sqrt{a}$, $b_7 = 2\sqrt{a}$, where the single number indicate the nature of a single existing fixed point, and the two numbers indicate the nature of both fixed points.

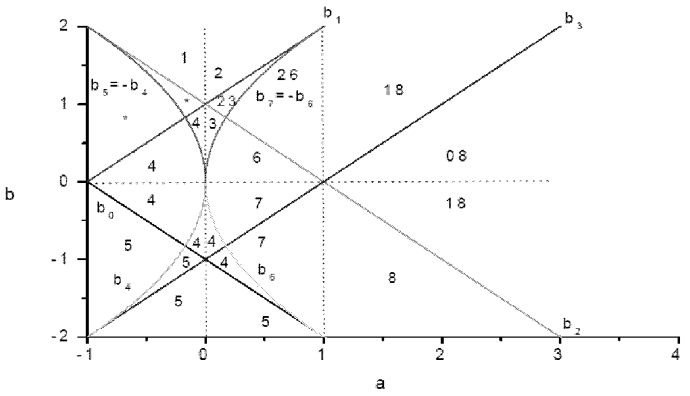

Figure 1 Stability of the fixed points of the map (3) in the ab-plane, where the numbers on the figure are as follow: 0: P_1 repeller, 1: P_1 regular saddle, 2: P_1 flip saddle, 3: P_2 regular attractor, 4: P_2 flip attractor, 5: P_2 flip saddle, 6: P_2 a clockwise spiral attractor, 7: P_2 a counter-clockwise spiral attractor, 8: P_2 repeller. * : There are no fixed points

3 Numerical Simulations

3.1 Observation of a New Chaotic Attractors

In this section, we illustrate some newly observed chaotic attractor, along with some other dynamical phenomena. The different chaotic attractors are shown in Figures 2–6 in black along with their basins of attraction in white.

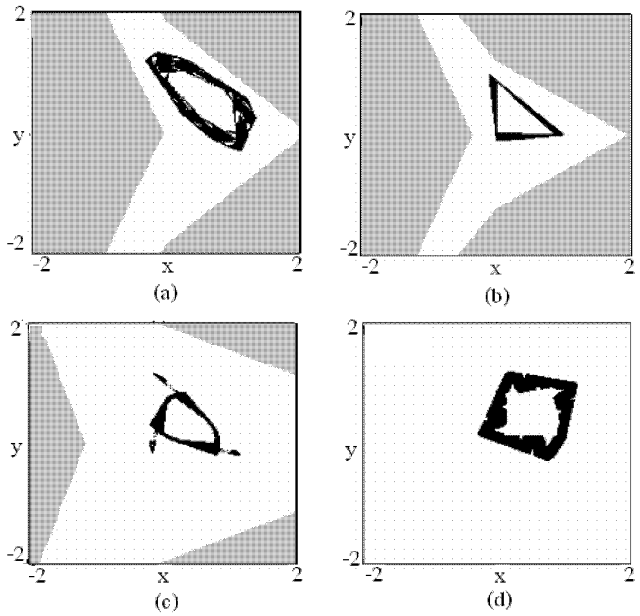

Figure 2 Chaotic attractors of the map (3) with their basins of attraction for $a = 1.1$ and (a) $b = -1.4$; (b) $b = -1.1$; (c) $b = 0.8$; (d) $b = 0.2$

In fact, the piecewise-linear (PWL) continuous chaotic systems can also generate various attractors, even the more complex multi-scroll attractors. As a note from the referee, it would be much better for the readers to know the recent advances in this topic. For PWL continuous sytems and multi-scroll attractors there is a large number of works including generation and circuit design for multi-scroll chaotic attractors[16–17]. Indeed, a family of n-double scroll chaotic attractors was introduced by Suykens and Vandewalle in [17]. Chaotic attractors with multiple-merged basins of attraction was studied by Lü, et al. in [18–19] using a switching manifold approach. In [20], Yalcin, et al. presented a family of scroll grid attractors by using a step function approach, including one-dimensional (1-D) n-scroll, two-dimensional (2-D) ($n \times m$)-grid scroll, and three-dimensional (3-D) ($n \times m \times l$)-grid scroll chaotic attractors. In [21–23], Lü et al. proposed rigorous theoretical proofs and experimental verifications the hysteresis series and saturated series methods for generating 1-D n-scroll, 2-D ($n \times m$)-grid scroll, and 3-D ($n \times m \times l$)-grid scroll chaotic attractors. In [24–25], Yu, et al., generates $2n$-wing and nxm-wing Lorenz-like attractors from a Lorenz-like systems and a modified Shimizu-Morioka model, respectively. Finally, using a thresholding approach, Lü, et al., generates multi-scroll chaotic attractors[26].

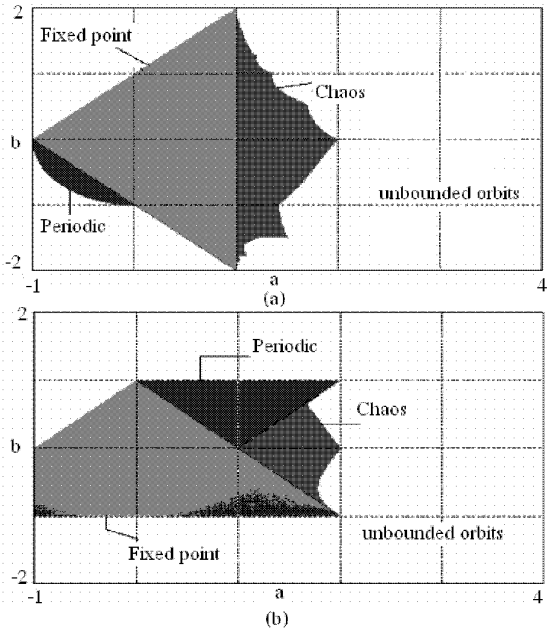

Figure 3 (a) Regions of dynamical behaviors in the ab-plane for the map (3); (b) Regions of dynamical behaviors in the ab-plane for the Lozi map (1)

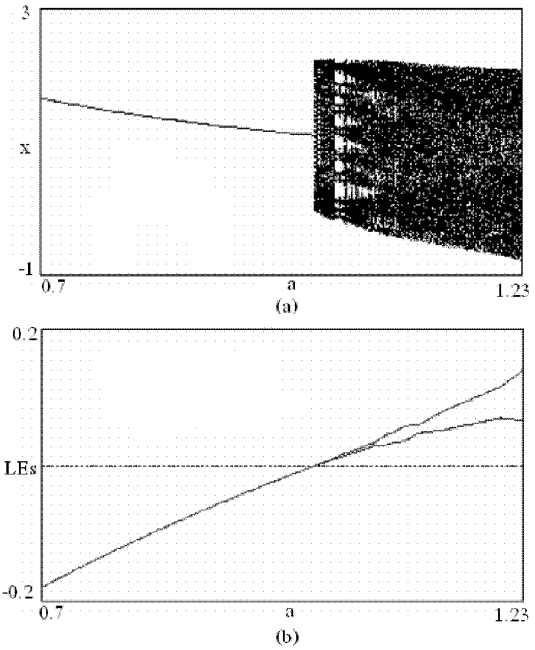

Figure 4 (a) The bifurcation diagram for the map (3) obtained for $b = 1.1$ and $0.7 \leq a \leq 1.23$; (b) Variation of the Lyapunov exponents of map (3) versus the parameter $0.7 \leq a \leq 1.23$, with $b = 1.1$

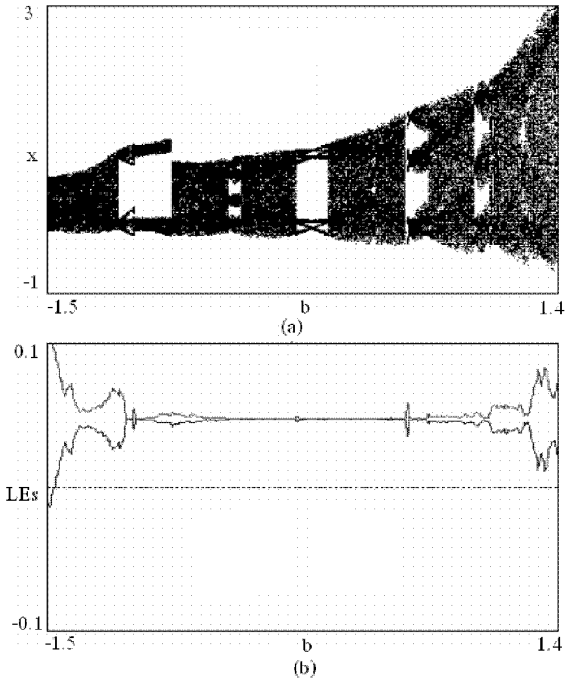

Figure 5 (a) The bifurcation diagram for the map (3) obtained for $a = 1.1$ and $-1.5 \leq b \leq 1.4$; (b) Variation of the Lyapunov exponents of map (3) versus the parameter $-1.5 \leq b \leq 1.4$, with $a = 1.1$

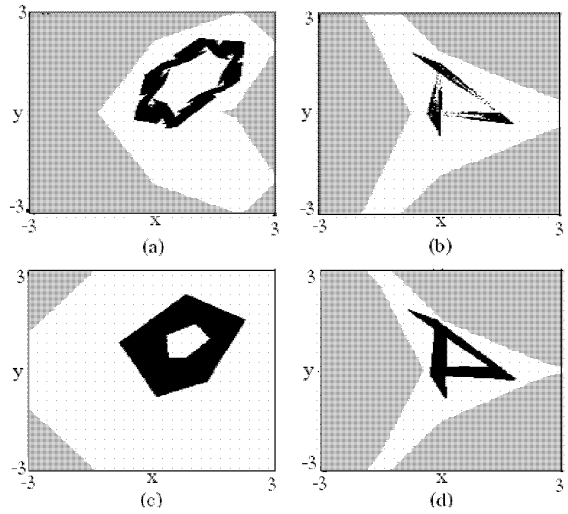

Figure 6 Chaotic attractors of the map (3) with their basins of attraction for (a) $a = b = 1.1$; (b) $a = 1.2, b = -1$; (c) $a = 1.2, b = 0.5$; (d) $a = 1.3, b = -1.1$

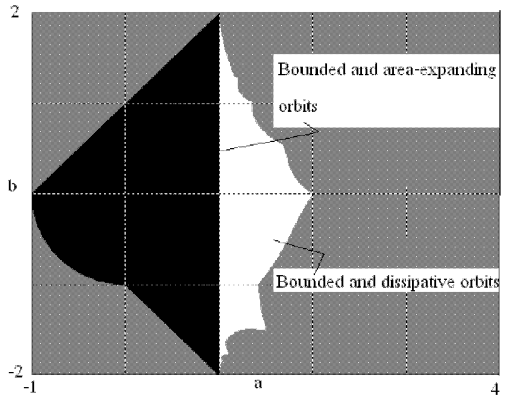

Figure 7 The sign of $\log|a|$ for the system (3) in the ab-plane defines the regions of net expansion and contraction

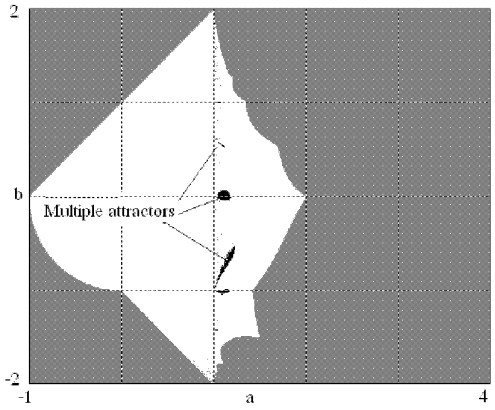

Figure 8 The regions of ab-space with multiple attractors (in black)

3.2 Route to Chaos

It is well-known that the Hénon map typically undergoes a period-doubling route to chaos as the parameters are varied. By contrast, the Lozi map[2] has no period-doubling route, but rather it goes directly into chaos from a border-collision bifurcation developed from a stable periodic orbit[3]. Similarly, the chaotic attractor given in [27] is obtained from a border-collision period-doubling bifurcation scenario. This scenario involves a sequence of pairs of bifurcations, whereby each pair consists of a border-collision bifurcation and a pitchfork bifurcation. Thus, the three chaotic systems go via different and distinguishable routes to chaos. Furthermore, the new piecewise linear chaotic attractor considered here results from a stable period-1 orbit to a fully developed chaotic regime. This particular type of bifurcation is called border collision bifurcation as shown in Figure 4 (a), and it is the only observed scenario.

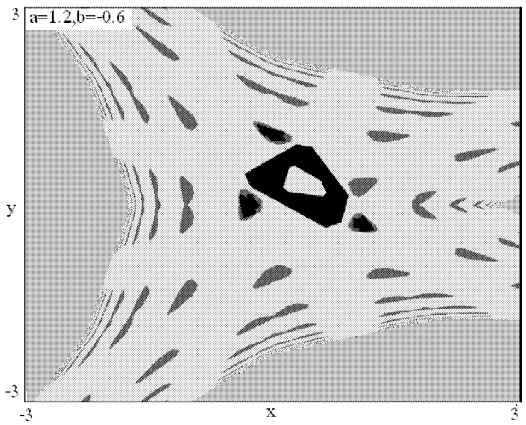

Figure 9 Coexisting attractors for the map (3) at $a = 1.2$ and $b = -0.6$, where the large chaotic attractor at the center (in black) is surrounded by a period-3 chaotic attractor at its periphery (also in black), with their basins of attraction shown in yellow and magenta, respectively

Figure 3 (a) shows regions of unbounded, fixed point, periodic, and chaotic solutions in the ab-plane for the map (3), where we use 10^6 iterations for each point. Note the agreement of Figure 3 with the bifurcation boundaries calculated above and plotted in Figure 1. For comparison, Figure 3 (b) shows a similar plot for the Lozi map (1). On the other hand, if we fix parameter $b = 1.1$ and vary $a \in \mathbb{R}$, the map (3) exhibits the following dynamical behaviors as shown in Figure 4: In the interval $a < 0.1$, the map (3) does not converge, for $0.1 \leq a < 1.01$, the map (3) converges to a fixed point. In the interval $1.01 \leq a \leq 1.23$, it converges to a hyper chaotic attractor (all Lyapunov exponents are positive) as shown in Figure 6 (a) . For $a > 1.23$, it does not converge.

Note that the sudden transition shown in Figure 4 (a) is not a new phenomenon. For example, it is also seen in the family of one-dimensional tent maps with the parameter giving the height of the tent.

However, if we fix parameter $a = 1.1$, and vary $b \in \mathbb{R}$, the map (3) exhibits the following dynamical behaviors as shown in Figure 5: For $b < -1.5$, and $b > 1.4$, it does not converge, and for $-1.5 \leq b < -1.4$, it converges to a chaotic attractor as shown in Figure 2 (a). For $-1.4 < b < 1.4$, it converges to a variety of hyper chaotic attractors as shown in Figures 2 and 6. One interesting feature is that this map is not dissipative for $|b| > 1$. In fact, there are values for which both Lyapunov exponents are positive as shown in Figures 4 (b) and 5 (b), indicating hyperchaos.

Since the map (3) is not everywhere dissipative, its attractor can have a dimension equal to or even greater than 2.0 by virtue of the folding afforded by the piecewise linearity. There are parameters such as $a = 1.1$ and $b = 1.1$ for which the two Lyapunov exponents are positive. Furthermore, when both Lyapunov exponents are positive, the dimension in principle could exceed 2.0, and this would be evident by examining the attractor in embeddings higher than 2. Takens' theorem[28] states that an embedding as large as $2D + 1$ might be necessary to resolve the overlaps.

As a test of this prediction, the correlation dimension was calculated with $a = b = 1.1$ for various embeddings using the extraplation method of Sprott and Rowlands[29], and the results shows the attractor dimension is apparently very close to 2 in all embeddings greater than 1. To

numerical precision (0.1), the correlation dimension appears to be very close to 2, presumably because the measure is uniform on the attractor, where the Lyapunov exponents in base-e (the natural logarithm function) are 0.057675 ± 0.012 and 0.037635 ± 0.012. Figure 7 shows the regions of the ab-plane where the system is dissipative and bounded (in white) and where it is dissipative but area-expanding (in black) as determined from the sign of $\log |a|$ (positive for $|a| \geq 1$, and negative for $|a| < 1$).

These results suggest that the Takens' criterion is applicable for the map (3) since the map is invertible for all $a \neq 0$, and hence there is a one-to-one reconstruction for the map (3). On the other hand, it is well-known that basin boundaries arise in dissipative dynamical systems when two or more attractors are present. In such situations each attractor has a basin of initial conditions that lead asymptotically to that attractor. The sets that separate different basins are called the basin boundaries. In some cases the basin boundaries can have very complicated fractal structure and hence pose an additional impediment to predict long-term behavior. For the map (3) we have calculated the attractors and their basins of attraction on a grid in ab-space where the system is chaotic. There is a wide variety of possible attractors, only some of which are shown in Figures 2–6. Also, numerical result indicate that most of the basin boundaries are smooth.

Note that the noisy region just above the $b = -1$ line for the Lozi map (1) in Figure 3(b) is actually a region of multiple attractors. For example, with $a = -0.9$ and $b = -0.9$, a period-5 attractor coexists with a fixed point (at $x = 1.0$); and with $a = 1$ and $b = -0.9$, a period-4 attractor coexists with a fixed point (at $x = 0.344828$).

Figure 8 was obtained by using 200 different random initial conditions and studying cases where the distribution of the average value of x on the attractor is bimodal. Since there is no rigorous test for bimodality, which was done by sorting the 200 values of $< x >$ and then dividing them into two equal groups. The group with the smallest range of $< x >$ was assumed to represent one of the attractors, and a second attractor was assumed to exist if the largest gap in the values of those in the other group was twice the range of the first group. The coexisting attractors where then confirmed in a separate calculation.

We remark from Figure 8 that coexisting attractors are evident in the chaotic region just above the line $a = 1$. Hence the robustness of chaos in the map (3) is lacking in these regions of the ab-plane since robust chaos is defined by the absence of periodic windows and coexisting attractors in some neighborhood of the parameter space, because the existence of these windows in some chaotic regions imply that small changes of the parameters would destroy the chaotic behavior. This effect implies the fragility of this type of chaos. Contrary to this situation, there are many practical applications as in communication and spreading the spectrum of switch-mode power supplies to avoid electromagnetic interference[30], where it is necessary to obtain reliable operation in the chaotic mode and robustness of chaos is required. A practical example can be found from electrical engineering to demonstrate robust chaos as shown in [8, 13–14]. If both Lyapunov exponents are positive throughout the range, then the resulting attractors are called hyper-chaotic, and they are clearly robust. For the cases $a = 1.1$, or $b = 1.1$ the map (3) displays a variety of hyper chaotic attractors as shown in Figures 2 and 6. The importance of these attractors is that they are more non-regular, and the iteration points are seemingly "almost" full of the considered space, which explains one of the applications of chaos in fluid mixing; for example, refer to [30].

We have verified the existence of coexisting chaotic attractors at $a = 1.2$ and $b = -0.6$ as shown in black in Figure 9. The large chaotic attractor at the center is surrounded by a period-3 chaotic attractor at its periphery, with their basins of attraction shown in yellow and magenta, respectively. The basin boundary is apparently fractal. This result is significant since there are relatively few simple 2-D piecewise linear maps that have coexisting chaotic attractors; for

example, see [31].

4 Conclusion

We have described a new simple 2-D discrete piecewise linear chaotic map. The detailed dynamical behaviors of this map were further investigated.

References

[1] R. L. Devaney, A piecewise linear model for the zones of instability of an area-preserving map, *Physica 10D*, 1984, 387–393.

[2] R. Lozi, Un attracteur étrange du type attracteur de Hénon, *Journal de Physique*, Colloque C5, Supplément au n^0 8, 1978, **39**: 9–10.

[3] Y. Cao and Z. Liu, Strange attractors in the orientation-preserving Lozi map, *Chaos Solitons Fractals*, 1998, **9**(11): 1857–1863.

[4] D. Aharonov, R. L. Devaney, U. Elias, The dynamics of a piecewise linear map and its smooth approximation, *International Journal of Bifurcation and Chaos*, 1997, **7**(2): 351–372.

[5] P. Ashwin and X. C. Fu, On the dynamics of some nonhyperbolic area-preserving piecewise linear maps, in Mathematics in Signal Processing V, Oxford Univ Press IMA Conference Series, 2002.

[6] J. Scheizer and M. Hasler. Multiple access communication using chaotic signals, in *Proc. IEEE ISCAS*'96, Atlanta, USA, 1996, **3**, 108.

[7] A. Abel, A. Bauer, K. Kerber, and W. Schwarz, Chaotic codes for CDMA application, in *Proc. ECCTD*'97, 1997, 1: 306.

[8] S. Banerjee and G. C. Verghese, *Nonlinear Phenomena in Power Electronics: Attractors, Bifurcations, Chaos, and Nonlinear Control*, IEEE Press, New York, 2001.

[9] S. Banerjee, S. Parui, and A. Gupta, Dynamical effects of missed switching in current-mode controlled dc-dc converters, *IEEE Trans. Circuits & Systems–II*, 2004, **51**: 649–654.

[10] R. Rajaraman, I. Dobson, and S. Jalali, Nonlinear dynamics and switching time bifurcations of a thyristor controlled reactor circuit, *IEEE Trans. Circuits & Systems–I*, 1996, **43**: 1001–1006.

[11] T. K. Tse, Complex behavior of switching power converters, CRC Press, Boca Raton, USA, 2003.

[12] M. di Bernardo, M. I. Feigin, S. J. Hogan, and M. E. Homer, Local analysis of Cbifurcations in n-dimensional piecewise smooth dynamical systems, *Chaos, Solitons & Fractals*, 1999, **10**(11): 1881–1908.

[13] S. Banergee, J. A. York, and C. Grebogi, Robust chaos, *Phys. Rev. Lettres*, 1998, **80**(14): 3049–3052.

[14] S. Banerjee, C. Grebogi, Border collision bifurcations in two-dimensional piecewise smooth maps, *Phys. Rev. E*, 1999, **59**: 4052–4061.

[15] M. A. Hassouneh, E. H. Abed, S. Banerjee, Feedback Control of border collision bifurcations in two-dimensional discrete-time systems, Technical Report, TR 2002-36, 2001.

[16] J. A. K. Suykens and J. Vandewalle, Generation of n–double scrolls ($n = 1, 2, \cdots$), *IEEE Trans. Circuits Syst. I, Fundam. Theory Appl.*, 1993, **40**(11): 861–867.

[17] S. M. Yu, J. H. Lu, W. K. S. Tang, and G. Chen, A general multiscroll Lorenz system family and its DSP realization, *Chaos*, 2006, **16**: 1–10.

[18] J. Lü, T. Zhou, G. Chen, and X. Yang, Generating chaos with a switching piecewise-linear controller, *Chaos*, 2002, **12**(2): 344–349.

[19] J. Lü, X. Yu, and G. Chen, Generating chaotic attractors with multiple merged basins of attraction: A switching piecewise-linear control approach, *IEEE Trans. Circuits Syst. I, Fundam. Theory Appl.*, 2003, **50**(2): 198–207.

[20] M. E. Yalcin, J. A. K. Suykens, J. Vandewalle, and S. Ozoguz, Families of scroll grid attractors, *Int. J. Bifurc. Chaos*, 2002, **12**(1): 23–41.

[21] J. Lü, F. Han, X. Yu, and G. Chen, Generating 3-D multi-scroll chaotic attractors: A hysteresis series switching method, *Automatica*, 2004, **40**(10): 1677–1687.
[22] J. Lü, G. Chen, X. Yu, and H. Leung, Design and analysis of multiscroll chaotic attractors from saturated function series, *IEEE Trans. Circuits Syst. I*, Reg. Papers, 2004, **51**(12): 2476–2490.
[23] J. Lü, S. M. Yu, H. Leung, and G. Chen, Experimental verification of multi-directional multi-scroll chaotic attractors, *IEEE Trans. Circuits Syst. I*, Reg. Papers, 2006, **53**(1): 149–165.
[24] S. M. Yu, W. K. S. Tang, J. Lü, and G. Chen, Generation of $n \times m$-wing Lorenz-like attractors from a modified Shimizu-Morioka model, *IEEE Transactions on Circuits and Systems II*, 2008.
[25] S. M. Yu, W. K. S. Tang, J. Lü, and G. Chen, Generating $2n$-wing attractors from Lorenz-like systems, *International Journal of Circuit Theory and Applications*, 2008.
[26] J. Lü, K. Murali, S. Sinha, H. Leung, and M. A. Aziz-Alaoui, Generating multi-scroll chaotic attractors by thresholding, *Physics Letters A*, 2008, **372**: 3234–3239.
[27] Zeraoulia Elhadj, A new chaotic attractor from 2-d discrete mapping via border-collision period doubling scenario, *Discrete Dynamics in Nature and Society*, 2005, **8**: 235–238.
[28] F. Takens, Detecting strange attractors in turbulence, *Lecture Notes in Mathematics*, Springer-Verlag, 1981, 898.
[29] J. C. Sprott and G. Rowlands, Improved correlation dimension calculation, *Int. J. Bifurcation. and Chaos*, 2001, **11**: 1865–1880.
[30] J. M. Ottino, F. J. Muzzion, M. Tjahjadi, et al., Chaos, symmetry, and self-similarity: Exploring order and disorder in mixing processes, *Science*, 1992, **257**: 754–760.
[31] M. Dutta, H. E. Nusse, E. Ott, et al., Multiple attractor bifurcations: A source of unpredictability in piecewise smooth systems, *Phys. Rev. Lett.*, 1999, **83**: 4281–4284.